Kuo, M. T., & Hsu, T. C. (1978) *Nature 271*, 83.
Ljungman, M. (1989) *Carcinogenesis 10*, 447.
Lorenz, J. D., Watkins, J. F., & Smerdon, M. J. (1988) *Mutat. Res. 193*, 167.
Miller, M. R., & Chinault, D. N. (1982) *J. Biol. Chem. 257*, 46.
Mosbaugh, D. W., & Linn, S. (1984) *J. Biol. Chem. 259*, 10247.
Nissen, K. A., Lan, S. Y., & Smerdon, M. J. (1986) *J. Biol. Chem. 261*, 8585.
Oleson, F. B., Mitchell, B. L., Dipple, A., & Lieberman, M. W. (1979) *Nucleic Acids Res. 7*, 1343.
Painter, R. B., & Young, B. R. (1971) *Mutat. Res. 14*, 225.
Pulleyblank, D. E., Shure, M., & Vinograd, J. (1977) *Nucleic Acids Res. 4*, 1409.
Regan, J. D., & Setlow, R. B. (1974) *Cancer Res. 34*, 3318.
Sancar, A., & Sancar, G. B. (1988) *Annu. Rev. Biochem. 57*, 29.
Seki, S., Ohashi, M., Ogura, H., & Oda, T. (1982) *Biochem. Biophys. Res. Commun. 104*, 1502.
Sidik, K., & Smerdon, M. J. (1984) *Carcinogenesis 5*, 245.
Sidik, K., & Smerdon, M. J. (1987) *Carcinogenesis 8*, 733.
Sidik, K., & Smerdon, M. J. (1990) *Cancer Res. 50*, 1613.
Smerdon, M. J. (1983) *Biochemistry 22*, 3516.
Smerdon, M. J. (1986) *J. Biol. Chem. 261*, 244.
Smerdon, M. J. (1989) in *DNA Repair Mechanisms and Their Biological Implications in Mammalian Cells* (Lambert, M. W., & Laval, J., Eds.) pp 271–294, Plenum Publishing Corp., New York.
Smerdon, M. J., & Lieberman, M. W. (1978) *Proc. Natl. Acad. Sci. U.S.A. 75*, 4238.
Smerdon, M. J., & Lieberman, M. W. (1980) *Biochemistry 19*, 2992.
Smerdon, M. J., Tlsty, T. D., & Lieberman, M. W. (1978) *Biochemistry 17*, 2377.
Smerdon, M. J., Kastan, M. B., & Lieberman, M. W. (1979) *Biochemistry 18*, 3732.
Smerdon, M. J., Lan, S. Y., Calza, R. E., & Reeves, R. (1982) *J. Biol. Chem. 257*, 13441.
Smith, C. A. (1987) *J. Cell Sci., Suppl. 6*, 225.
Smith, C. A., Cooper, P. K., & Hanawalt, P. C. (1981) in *DNA Repair: A Laboratory Manual of Research Procedures* (Friedberg, E. C., & Hanawalt, P. C., Eds.) Vol. 1B, pp 289–305, Marcel Dekker Inc., New York.
Snyder, R. D., & Regan, J. D. (1982) *Carcinogenesis 3*, 7.
Stubbe, J., & Kozarich, J. W. (1987) *Chem. Rev. 87*, 1107.
Th'ng, J. P. H., & Walker, I. G. (1985) *Mutat. Res. 165*, 139.
Tlsty, T. D., & Lieberman, M. W. (1978) *Nucleic Acids Res. 5*, 3261.
Uesugi, S., Shida, T., Ikehara, M., Kobayashi, Y., & Kyogoku, Y. (1984) *Nucleic Acids Res. 12*, 1581.
Villeponteau, B., & Martinson, H. G. (1987) *Mol. Cell. Biol. 7*, 1917.
Walker, I. G., & Th'ng, J. P. H. (1982) *Mutat. Res. 105*, 277.
Willis, C. E., & Holmquist, G. P. (1985) *Electrophoresis 6*, 259.
Zolan, M. E., Smith, C. A., Calvin, N. M., & Hanawalt, P. C. (1982) *Nature 299*, 462.

# Effect of Central-Residue Replacements on the Helical Stability of a Monomeric Peptide†

Gene Merutka, William Lipton, William Shalongo, Soon-Ho Park, and Earle Stellwagen*
*Department of Biochemistry, University of Iowa, Iowa City, Iowa 52242*
*Received April 3, 1990; Revised Manuscript Received May 8, 1990*

ABSTRACT: The peptide acetylYEAAAKEARAKEAAAKAamide exhibits the dichroic features characteristic of a monomeric helix/coil transition in aqueous solution. Nineteen variants of this peptide each containing a different residue at position 9 were prepared by solid-phase peptide synthesis and purified by reversed-phase chromatography. The thermal dependence of the far-ultraviolet dichroic spectrum of each of these peptides except that containing proline is characteristic for an $\alpha$-helix/coil transition. The relative stability of the helical forms of these peptides does not correlate with the preference of the variable amino acid to occupy a middle position in a protein helix. It is likely that the specific interactions of the variable residue with its local environment obscure any inherent preference of the residue to reside in an $\alpha$-helix.

Baldwin and his associates (Marqusee & Baldwin, 1987; Shoemaker et al., 1987) have demonstrated that peptides containing fewer than 20 residues can be designed to exhibit a significant population of helical residues in aqueous solution. In this paper, we have altered one of their designed peptides, acetylAEAAAKEAAAKEAAAKAamide, to investigate the effect of residue replacement on the population of helical residues. The alanine residue at position 1 was replaced with a tyrosine to increase the precision and rapidity of the measurement of peptide concentration. The central alanine residue was selected for replacement by each of the other 19 residues to minimally perturb both the helix dipole and the three potential salt bridges in the designed peptide. Accordingly, each peptide considered in this paper has the sequence acetyl-YEAAAKEAXAKEAAAKAamide and will be designated by the residue at position X with the one-letter code. The effect of each central-residue replacement on the population of helical residues was measured by circular dichroism, and the results are compared with the preference of each residue

† This investigation was supported by Public Health Service Program Project Grant HE 14388 from the National Heart, Lung and Blood Institute and by National Science Foundation Biological Instrumentation Program Grant DMB 8413658.

0006-2960/90/0429-7511$02.50/0 

to occupy a central position of a helix in a globular protein.

## Materials and Methods

*Peptide Synthesis and Characterization.* The peptides described in this paper were obtained from the simultaneous multiple peptide synthesis procedure (Houghten et al., 1986), fractionated by reversed-phase chromatography, and characterized as described previously (Merutka & Stellwagen, 1990). Analytical reversed-phase chromatography was performed on a 4.6 × 100 mm $C_{18}$ Spherisorb ODS2 column containing 3-μm particles with approximately 120000 plates/m. Peptide samples were partitioned in a linear gradient between 10% and 40% acetonitrile in 0.1% trifluoroacetic acid. The gradient was generated in 25 min with a flow rate of 1 mL/min at ambient temperature. The chromatographic elution profile observed for each peptide is characterized by a single peak, which accounted for at least 90% of the material eluted by the gradient. The retention times for the individual peptides correspond very well with the retention times predicted (Houghten & DeGraw, 1987) for members of a homologous series having a single variable residue. The mass/charge ratio of the main molecular ion of each peptide observed by mass spectrometry is within 1 mass unit of that expected for each singly protonated peptide. Finally, amino acid compositional ratios of each peptide are in excellent agreement with the ratios expected.

*Spectral Measurements.* All spectral measurements were made with stoppered Hellma optical cells having a path length of either 1 or 10 mm and solutions containing 10 mM NaCl and 1 mM phosphate buffer, pH 7.0, except where noted otherwise. Solutions of peptides containing either cysteine or methionine included 0.5 mM dithiothreitol. Absorbance measurements were made on either a Gilford Response II or an Aviv Associates Model 14DS spectrophotometer. Circular dichroism measurements were made as described previously (Merutka & Stellwagen, 1990) on an Aviv Associates Model 60DS spectropolarimeter. Each solution was equilibrated at a given temperature until the ellipticity at 222 nm was constant prior to the recording of dichroic measurements. All ellipticity measurements are expressed as mean residue ellipticity, $[\theta]$, having the units deg cm$^2$ dmol$^{-1}$. The ellipticity of each peptide solution at 222 nm and 0 °C was recovered within 200 deg cm$^2$ dmol$^{-1}$ upon heating the solution to 85–95 °C and cooling to 0 °C. Repetitive measurements of different solutions of a given peptide gave an average difference in ellipticity of 600 deg cm$^2$ dmol$^{-1}$ at 222 nm and 0 °C.

*Peptide Concentration.* The concentration of each peptide was calculated from the difference absorption spectrum generated by the phenolic ionization of the terminal tyrosine residue. Difference spectra obtained at ambient temperature between pH 13 and pH 7 exhibited maxima at 243 and 295 nm and minima at 222 and 274 nm, each with an experimental variance of 1 nm. Peptide concentration was calculated from such difference spectra with a difference extinction of 11 100 M$^{-1}$ cm$^{-1}$ at 243 nm (Mihalyi, 1968).

*Analysis of Dichroic Transitions.* The thermal dependence of the ellipticity of each peptide at 222 nm was analyzed on an Apollo Domain Series 3500 computer. The analysis assumes that thermal dependence of each peptide can be described by a two-state transition involving the helix, H, and coil, C, forms of each peptide and that all of the residues are either in a helix or a coil. The transition is written in the direction of helix formation C ⇄ H, giving the equilibrium constant expression in eq 1, where $[\theta]$ is the observed ellipticity,

$$K = [\mathrm{H}]/[\mathrm{C}] = ([\theta] - [\theta]_\mathrm{C})/([\theta]_\mathrm{H} - [\theta]) \qquad (1)$$

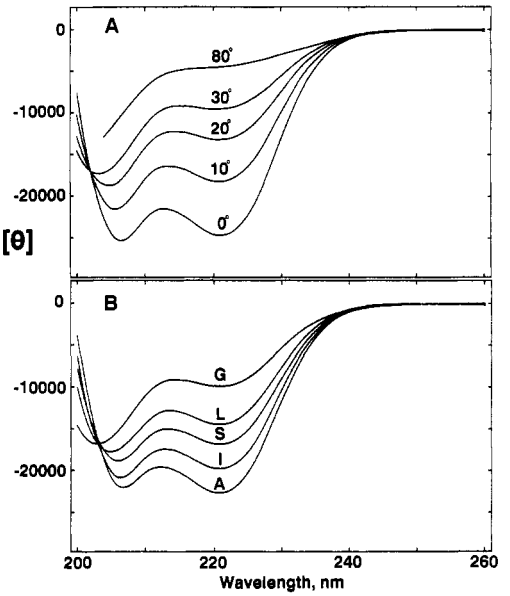


FIGURE 1: Circular dichroic spectra of peptides. Panel A illustrates the dichroic spectrum of a 29 μM solution of peptide R at the indicated temperatures. Panel B illustrates the dichroic spectra for 24–49 μM solutions of peptides A, G, I, L, and S observed at 0 °C. All peptide solutions contained 10 mM NaCl and 1 mM phosphate buffer, pH 7.0.

$[\theta]_\mathrm{H}$ is the ellipticity of the helical form of the peptide, and $[\theta]_\mathrm{C}$ is the ellipticity of the coil form of the peptide. The thermal dependence of the observed ellipticity is assumed to be described by the van't Hoff relationship, eq 2, in which $T_\mathrm{m}$

$$K = \exp[-\Delta H°/R(1/T - 1/T_\mathrm{m})] \qquad (2)$$

is the temperature at the midpoint of the transition where $K = 1$. The computer is programmed to identify the combination of $[\theta]_\mathrm{H}$, $[\theta]_\mathrm{C}$, $T_\mathrm{m}$, and $\Delta H°$ values that generates the smallest $\chi^2$ deviation from the measured ellipticity values. A $\Delta G°$ and thus a $\Delta S°$ can then be obtained at any temperature from these values. The program can also fit the measured ellipticity to eqs 1 and 2 by holding one or more of the variables to preselected values. In this paper, most of the fitting was done with a constant difference between ellipticity of the helical and coil forms of the peptide.

## Results and Discussion

All dichroic measurements reported here were obtained with peptide concentrations of between 15 and 50 μM. The mean residue molar ellipticity at 222 nm and 0 °C is −12000 ± 400 deg cm$^2$ dmol$^{-1}$ for peptide W, over the concentration range 10–400 μM, and is −22200 ± 400 deg cm$^2$ dmol$^{-1}$ for peptide R, over the concentration range 10–100 μM. It has previously been reported (Merutka & Stellwagen, 1990) that the ellipticity of peptides of similar sequence containing alanine, methionine, or serine replacements at variable position X is independent of peptide concentration up to 400 μM. Such consistency exhibited by peptides containing quite different residues suggests that peptide association is not a significant factor in these measurements.

The far-ultraviolet circular dichroic spectrum of peptide R observed at neutral pH and 0 °C is bimodal with minima at 207 and 222 nm as illustrated in Figure 1A. Such spectra are commonly interpreted to indicate the presence of a significant population of residues in the α-helical conformation (Holzwarth & Doty, 1965). As the temperature of the solution of peptide R is raised, the bimodal spectrum is gradually converted into a relatively featureless spectrum as shown in

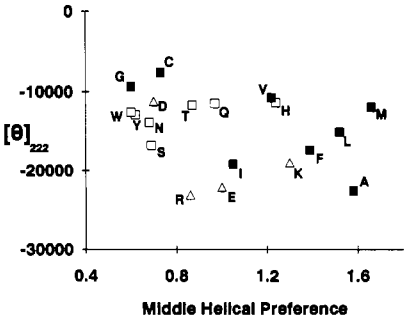


FIGURE 2: Correlation of peptide ellipticity with helix preference. The ordinate is the measured mean residue ellipticity of each peptide except P at 222 nm and 0 °C in 10 mM NaCl and 1 mM phosphate buffer, pH 7.0. The abscissa is the relative preference of the variable residue in the peptide for the middle of a protein helix (Argos & Palau, 1982). The filled squares indicate residues with no polar atoms, the open squares indicate residues with polar uncharged side chains, and the open triangles denote residues with charged side chains.

Figure 1A. The featureless spectrum observed at 90 °C is similar to that observed for a variety of unfolded proteins in excess denaturant at ambient temperature (Cortijo et al., 1973; Rossi et al., 1983; Rudolph et al., 1986). We will consider such a spectrum to indicate the absence of any regular structure and designate such residues as being in the coil form. The appearance of an isodichroic value at 202 nm in the spectra of peptide R observed below 35 °C suggests that the spectral changes caused by increasing the temperature can be considered a two-state $\alpha$-helix/coil transition of each peptide residue. Unfortunately, the isodichroic value cannot be observed at higher temperatures because of the increased absorbance of the solvent. The ellipticity at 222 nm describes a smooth dependence on temperature, suggesting that the residues in peptide R simultaneously change their fractional helix population with temperature. Accordingly, we will consider the dichroic changes with temperature to indicate changes in the helicity of the entire peptide as opposed to changes in the helicity of individual residues within the peptide.

The far-ultraviolet dichroic spectrum of each of the peptides except P is bimodal at neutral pH and 0 °C, having one minimum at 222 ± 1 nm and a second minimum located between 203 and 207 nm, as shown in Figure 1B. These spectra form an isodichroic value at 202 nm similar to the isodichroic value observed upon heating peptide R. This correspondence suggests that both temperature and the residue occupying the central position can perturb the two-state helix/coil transition of a peptide. Accordingly, the ellipticity of each peptide at a fixed wavelength and temperature should indicate the relative ability and the central residue to stabilize the peptide helix. We have chosen to use the ellipticity at 222 nm and 0 °C, which range from −7700 deg cm$^2$ dmol$^{-1}$ for peptide C to −23 100 deg cm$^2$ dmol$^{-1}$ for peptide R. These ellipticity values are plotted in Figure 2 against the preference of each residue to occupy a central position in a protein helix obtained from statistical analysis of crystallographic models (Argos & Palau, 1982). The two data sets appear unrelated, having a linear correlation coefficient of −0.31. Alternative statistical helix preference values (Chou & Fasman, 1974a,b; Levitt, 1978; Richardson & Richardson, 1988) generate correlation coefficients ranging from −0.29 to −0.38. Use of Zimm−Bragg $\sigma$ values at 0 °C obtained from host−guest studies of random copolymers (Sueki et al., 1984; Vasquez et al., 1987) generates correlation coefficients ranging from −0.30 to −0.34.

Very recently, Padmanabhan et al. (1990) have compared the ellipticity values of a series of monomeric peptides in which

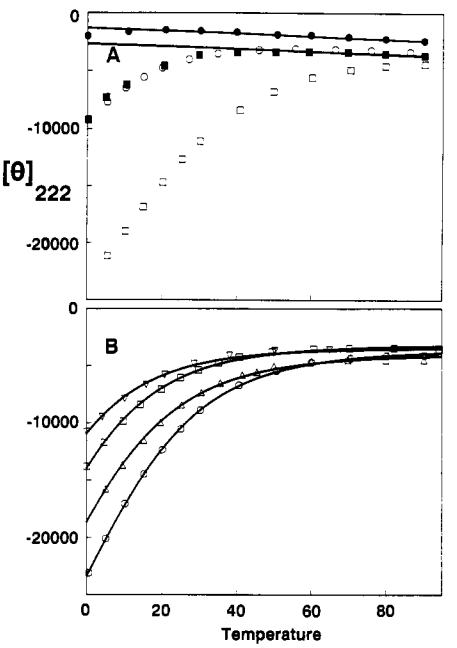


FIGURE 3: Dependence of peptide ellipticity at 222 nm on temperature. Panel A illustrates the thermal dependence of peptides A and G observed at elevated temperatures. The circles denote values for a 26 $\mu$M solution of peptide G, and the squares denote values for a 49 $\mu$M solution of peptide A. The open symbols indicate values obtained in solutions containing 10 mM NaCl, and the filled symbols indicate values obtained in solution containing 5.0 M NaCl. All solution contained 1 mM phosphate buffer, pH 7.0. Panel B illustrates the thermal dependence of the mean residue ellipticity at 222 nm for peptides V (▽), N (□), K (△), and R (○) in 10 mM NaCl and 1 mM phosphate buffer, pH 7.0. These ellipticity values have been corrected for the thermal coefficient of the coil form as described in the text. All lines were simulated by assuming a difference in ellipticity of the helix and coil form of each peptide of 35 300 deg cm$^2$ dmol$^{-1}$. The line for peptide K was simulated with an ellipticity value for the coil form of −3970 deg cm$^b$ dmol$^{-1}$, a melting temperature of −4.8 °C, and a $\Delta H°$ of 10.2 kcal mol$^{-1}$. Corresponding values for the line simulating the thermal transition of peptide N were −3180, −11.2, and 10.4; for peptide R, −3640, 3.3, and 10.8; and for peptide V, −3430, −17.6, and 10.3, respectively.

alanine residues are systematically replaced with phenylalanine, valine, isoleucine, and leucine residues. The sign and magnitude of the difference ellipticity observed here between peptide A and peptides F, V, and I are very similar to those of the difference ellipticity observed per replacement by Padmanabhan et al. However, the difference ellipticity for peptide L observed here is much larger than that reported by Padmanabhan et al. This discrepancy may be related to the unusual pH profile for peptide L, which is described below.

Since comparison of ellipticity values at a single temperature could be misleading, we measured the effect of temperature on the dichroic spectrum of each of the peptides. Increasing the temperature of each peptides solution except that of P generated a spectral change characteristic of a two-state $\alpha$-helix/coil transition. The thermal spectra of each of these peptides have an isodichroic point at 202 ± 1 nm at temperatures below 35 °C having a mean ellipticity of −14 800 deg cm$^2$ dmol$^{-1}$ with a standard deviation of 1600. The ellipticity at 222 nm of each peptide solution decreases regularly with increasing temperature, as illustrated in Figure 3A by peptide A in 0.01 M NaCl. However, peptides with relatively little helicity at 0 °C attain a maximal ellipticity value at 222 nm which then decreases linearly with further increase in temperature, as illustrated in Figure 3A by peptide G in 0.01 M NaCl. Increasing the concentration of NaCl to 5.00 M extends the thermal range over which the linear decrease in ellipticity

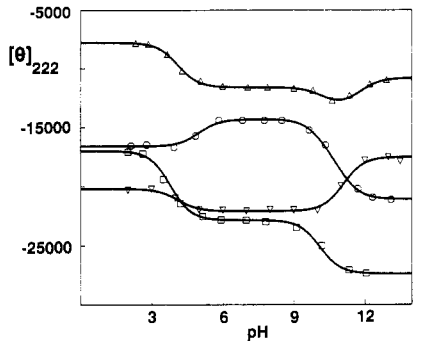


FIGURE 4: Dependence of peptide ellipticity at 222 nm and 0 °C on pH. Each peptide was dissolved in a solution containing 10 mM NaCl and 1 mM phosphate buffer, pH 7.0. The pH of the solution was first decreased by stepwise addition of HCl and then returned to neutral pH by addition of KOH, and then the pH was increased by stepwise addition of KOH. The profiles depicted are for peptides T (△), L (○), R (□), and E (▽).

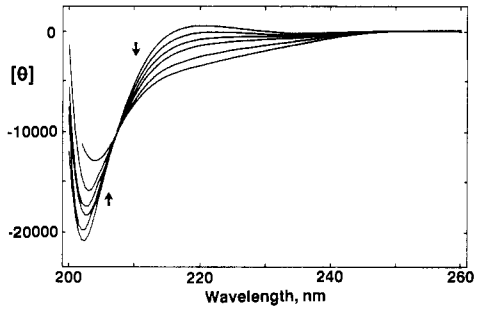


FIGURE 5: Circular dichroic spectra of peptide P. Spectra displayed were obtained with a 49 μM solution of peptide P in 10 mM NaCl and 1 mM phosphate buffer, pH 7.0, at 0, 10, 20, 30, 50, and 70 °C. The arrows indicate changes in the spectra with increasing temperature.

is observed for peptide G and reveals this phenomenon for peptide A, as illustrated in Figure 3A. The linear decrease in ellipticity with increasing temperature observed for six peptides has a mean value of −13 deg cm$^2$ dmol$^{-1}$ per degree of temperature increase at 222 nm. We suggest that this represents the thermal coefficient for the coil form of each peptide.

The thermal dependence of the corrected ellipticity at 222 nm of each peptide except peptide P can be fit with a sigmoidal curve by the van't Hoff equation as described under Materials and Methods. Examples of fitted transitions are illustrated in Figure 3B. For purposes of comparison, we have assumed that the difference in the mean residue ellipticity of the helix and coil form of each peptide has the same value as that obtained with peptide R, 35 300 deg cm$^2$ dmol$^{-1}$. With this assumption, the helical form of each peptide has an average mean residue ellipticity of −38 000 deg cm$^2$ dmol$^{-1}$ and the coil form a value of −2760 deg cm$^2$ dmol$^{-1}$, each with a standard deviation of 980. This consistency suggests that the thermal transitions of the 19 peptides can be treated, to a first approximation, as a homologous series with different melting temperatures. The melting temperatures of the individual peptides range from −19 °C for peptide C to +3 °C for peptide R. Replacement of the ellipticity values for each peptide at 222 nm and 0 °C with either the melting temperature of each peptide or its $\Delta G°$ at 0 °C does not significantly alter the relationship illustrated in Figure 2. Accordingly, the ellipticity values measured at 0 °C appear to provide a reliable index of fractional helicity.

The fitted thermal transitions also indicate the helix/coil transition of each peptide has a mean $\Delta H°$ of 9.7 kcal mol$^{-1}$ with a standard deviation of 1.2. Combination of the observed $\Delta H°$ with the $\Delta G°$ at 0 °C for the fitted helix/coil transition of each peptide gives a mean $\Delta S°$ of −37 cal deg$^{-1}$ mol$^{-1}$ with a standard deviation of 5. Accordingly, replacement of the central residue appears to perturb both the enthalpic and entropic aspects to the helix/coil transition to a similar degree.

We suggest that the local environment of a residue can significantly perturb any inherent preference the residue may have for a helical structure. The pH dependence observed for the individual peptides at 222 nm and 0 °C describes at least four distinct profiles, which are illustrated in Figure 4. Similar profiles have been observed by changing the spacing or the order of the glutamate/lysine pairs while retaining the same amino acid composition (Marqusee & Baldwin, 1987). The spectral changes accompanying the pH transitions illustrated in Figure 4 are characteristic for changes in the helix/coil equilibrium. These observations suggest that the variable residue can perturb the electrostatic interactions within a peptide, that different residues produce markedly different perturbations, and that each of these perturbations is coupled with the helix/coil equilibrium. The coupling of particular local interactions with the helix/coil equilibrium would then perturb expression of any inherent preference of a residue for an α-helix. We suggest the abscissa in Figure 2 represents the helix preference of a residue in an averaged environment while the ordinate represents the helix preference of a residue in a particular environment, namely, that about residue X in the peptide acetylYEAAAKEAXAKEAAAKAamide. A detailed analysis of the pH profiles of these peptides is currently in progress.

The residue at position X may also effect the kind of helix that is preferentially stabilized. Comparisons of the spectra in Figures 1 and 5 clearly indicate that peptide P contains little if any α-helicity at 0 °C and neutral pH. This suggests that proline interrupts helix formation and that the two flanking segments, each containing eight residues, are unable to stabilize shortened α-helices. In support of this suggestion, we find that the peptide acetylAEAAAKAamide has a dichroic spectrum at 0 °C characteristic for the coil form (Merutka and Stellwagen, unpublished results). As the temperature of the solution of peptide P is raised, its dichroic spectrum begins to resemble that of a coil form, as shown in Figure 5. This transformation is accompanied by a clear isodichroic point, indicating a two-state structural transition. However, the occurrence of the isodichroic point at 207 instead of 202 nm further indicates that an α-helix is not the structured form. Both the shape of the dichroic spectrum of peptide P and its dependence on temperature are similar to those of the corresponding spectra for the left-handed poly(L-proline) II helix (Tiffany & Krimm, 1968, 1972; Drake et al., 1988). If this comparison is valid, the central residue may influence the population of a variety of regular structures of similar stability.

## ACKNOWLEDGMENTS

We thank the personnel in the University of Iowa Protein Structure Facility and High Resolution Mass Spectrometry Facility for their analytical results.

## REFERENCES

Argos, P., & Palau, J. (1982) *Int. J. Pept. Protein Res. 19*, 380–393.

Chou, P. Y., & Fasman, G. D. (1974a) *Biochemistry 13*, 211–222.

Chou, P. Y., & Fasman, G. D. (1974b) *Biochemistry 13*, 222–245.

Cortijo, M., Panijpan, B., & Gratzer, W. B. (1973) *Int. J. Pept. Protein Res. 5*, 179–186.

Drake, A. F., Siligardi, G., & Gibbons, W. A. (1988) *Biophys. Chem. 31*, 143-146.
Holzwarth, G., & Doty, P. J. (1965) *J. Am. Chem. Soc. 87*, 218-228.
Houghten, R. A., & DeGraw, S. T. (1987) *J. Chromatogr. 386*, 223-228.
Houghten, R. A., DeGraw, S. T., Bray, M. K., Hoffman, S. R., & Frizzell, N. D. (1986) *Biochemistry 4*, 522-528.
Levitt, M. (1978) *Biochemistry 17*, 4277-4285.
Marqusee, S., & Baldwin, R. L. (1987) *Proc. Natl. Acad. Sci. U.S.A. 84*, 8898-8902.
Merutka, G., & Stellwagen, E. (1990) *Biochemistry 29*, 894-898.
Mihalyi, E. (1968) *J. Chem. Eng. Data 13*, 179-182.
Padmanabhan, S., Marqusee, S., Ridgeway, T., Laue, T. M., & Baldwin, R. L. (1990) *Nature (London) 344*, 268-270.
Richardson, J. A., & Richardson, D. C. (1988) *Science 240*, 1648-1652.
Rossi, V., Grandi, C., Dalzoppo, D., & Fontana, A. (1983) *Int. J. Pept. Protein Res. 22*, 239-250.
Rudolph, R., Fuchs, I., & Jaenicke, R. (1986) *Biochemistry 25*, 1662-1669.
Shoemaker, K. R., Kim, P. S., York, E. J., Stewart, J. M., & Baldwin, R. L. (1987) *Nature (London) 326*, 563-567.
Sueki, M., Lee, S., Powers, S. P., Denton, J. B., Konishi, Y., & Scheraga, H. A. (1984) *Macromolecules 17*, 148-155.
Tiffany, M. L., & Krimm, S. (1968) *Biopolymers 6*, 1379-1382.
Tiffany, M. L., & Krimm, S. (1972) *Biopolymers 11*, 2309-2316.
Vasquez, M., Pincus, M. R., & Scheraga, H. A. (1987) *Biopolymers 26*, 351-371.

# Sequence-Specific $^1$H NMR Assignments and Determination of the Secondary Structure for the Activation Domain Isolated from Pancreatic Procarboxypeptidase B†

Josep Vendrell,‡ Gerhard Wider,‡ Francesc X. Avilés,§ and Kurt Wüthrich*,‡

*Institut für Molekularbiologie und Biophysik, Eidgenössische Technische Hochschule—Hönggerberg, CH-8093 Zürich, Switzerland, and Departament de Bioquímica i Biologia Molecular, Unitat de Ciències, Universitat Autònoma de Barcelona, 08193 Bellaterra (Barcelona), Spain*

*Received January 25, 1990; Revised Manuscript Received April 18, 1990*

ABSTRACT: Nearly complete sequence-specific $^1$H NMR assignments are presented for amino acid residues 3-81 in the 81-residue globular activation domain of porcine pancreatic procarboxypeptidase B isolated after limited tryptic proteolysis of the zymogen. These resonance assignments are consistent with the chemically determined amino acid sequence. Regular secondary structure elements were identified from nuclear Overhauser effects and the sequence locations of slowly exchanging backbone amide protons. The molecule contains two $\alpha$-helices, including residues 20-30 and approximately residues 58-72, and a three-stranded antiparallel $\beta$-sheet with the individual strands extending approximately from 12 to 17, 50 to 55, and 75 to 77. The identification of these secondary structures and a preliminary analysis of additional long-range NOE distance constraints show that isolated activation domain B forms a stable structure with the typical traits of a globular protein. The data presented here are the basis for the determination of the complete three-dimensional structure of activation domain B, which is currently in progress.

Procarboxypeptidases are the inactive precursors of carboxypeptidases, a class of proteolytic enzymes that degrade polypeptides from their carboxy terminal. Two of these zymogens, A and B, are named after the corresponding active enzymes, which are classified according to their specificity for cleaving certain C-terminal peptide bonds. Upon activation by limited proteolysis, the zymogens are converted into the active enzymes through the release of a polypeptide of about 90-100 amino acid residues (Quinto et al., 1982; Vendrell et al., 1986; Flogizzo et al., 1988; Wade et al., 1988; Gardell et al., 1988; Clauser et al., 1988). This activation segment[1] has been shown to play an essential role in inhibiting the catalytic activity of the protein in its zymogen state (San Segundo et al., 1982), probably by blocking the interaction between substrates and the preformed catalytic site (Uren & Neurath, 1974). The so far unanswered question then arises whether the function of the activation segment depends on the formation of a defined tertiary structure in the proenzyme. In

† Financial support for this project was obtained from the Schweizerischer Nationalfonds (Project 31.25174.88), CICYT (Ministerio de Educación y Ciencia, Spain, Project BIO88/0456), and EMBO (long-term postdoctoral fellowship to J.V.).

‡ Eidgenössische Technische Hochschule—Hönggerberg.
§ Universitat Autònoma de Barcelona.

[1] Abbreviations: NMR, nuclear magnetic resonance; 2D, two dimensional; Bis-Tris, [bis(2-hydroxyethyl)amino]tris(hydroxymethyl)-methane; 2QF-COSY, two-dimensional two-quantum filtered correlation spectroscopy; 2Q spectra, two-dimensional two-quantum spectroscopy; TOCSY, two-dimensional total correlation spectroscopy; NOE, nuclear Overhauser effect; NOESY, two-dimensional NOE spectroscopy; activation domain B, trypsin-resistant N-terminal 81-residue portion of the activation segment isolated from porcine pancreatic procarboxypeptidase B; activation segment A, activation segment isolated from porcine pancreatic procarboxypeptidase A; $d_{AB}(i,j)$, distance between proton types A and B located in amino acid residues $i$ and $j$, respectively, where N, $\alpha$, and $\beta$ denote the amide proton, $C^{\alpha}H$, and $C^{\beta}H$, respectively.

0006-2960/90/0429-7515$02.50/0 